Steric Interactions of Valines 1, 5, and 7 in [Valine 5, D-Alanine 8] Gramicidin A Channels

Anthony R. Jude, Denise V. Greathouse, Marvin C. Leister, and Roger E. Koeppe II
Department of Chemistry & Biochemistry, University of Arkansas, Fayetteville, Arkansas 72701 USA

ABSTRACT When the central valine residues 6, 7, and 8 of gramicidin A (gA) are shifted by one position, the resulting [Val^5, D-Ala^8]gA forms right-handed channels with a single-channel conductance and average duration somewhat less than gA channels. The reduction in channel duration has been attributed to steric conflict between the side chains of Val^1 and Val^5 in opposing monomers (Koeppe, R. E. II, D. V. Greathouse, A. Jude, G. Saberwal, L. L. Providence, and O. S. Andersen. 1994. *J. Biol. Chem.* 269:12567–12576). To investigate the orientations and motions of valines in [Val^5, D-Ala^8]gA, we have incorporated ^{2}H labels at Val 1, 5, or 7 and recorded ^{2}H-NMR spectra of oriented and nonoriented samples in hydrated dimyristoylphosphatidylcholine. Spectra of nonoriented samples at 4°C reveal powder patterns that indicate rapid side chain "hopping" for Val^5, and an intermediate rate of hopping for Val^1 and Val^7 that is somewhat slower than in gA. Oriented samples of deuterated Val^1 and Val^7 show large changes in the methyl and C_β-^{2}H quadrupolar splittings ($\Delta\nu_q$) when Ala^5 in native gA is changed to Val^5. Three or more peaks for the Val^1 methyls with $\Delta\nu_q$ values that vary with the echo delay, together with an intermediate spectrum for nonoriented samples at 4°C, suggest unusual side chain dynamics for Val^1 in [Val^5, D-Ala^8]gA. These results are consistent with a steric conflict that has been introduced between the two opposing monomers. In contrast, the acylation of gA has little influence on the side chain dynamics of Val^1, regardless of the identity of residue 5.

INTRODUCTION

The ability to predict the effects of individual or multiple amino acid sequence modifications on the structure and function of peptides is a key step toward the de novo design of functional proteins (Koeppe and Andersen, 1996). To be able to predict the folding and conformation of a sequence of amino acids, one must first determine how individual amino acids will respond to the environment in which they are placed. Important interactions may occur with the surrounding environment including neighboring amino acids, and/or with residues that are distant in sequence but come in close proximity during the folding of the peptide. A peptide with a well-defined structure and function can be used as a model to study how changes in the primary sequence may alter its properties.

Gramicidin A channels have a well-defined structure and function (for reviews, see Andersen and Koeppe, 1992; Killian, 1992; Cardew, 1999), and serve as an excellent model to examine the effects of single and multiple sequence modifications (Durkin et al., 1990; Becker et al., 1991, 1992; Koeppe et al., 1994a; Salom et al., 1995, 1998; Jude et al., 1999). Gramicidin channels assemble in membranes or membrane-like environments by the association of two monomers that emanate from opposite sides of a lipid bilayer (O'Connell et al., 1990). Each gA monomer consists of 15 alternating L- and D-amino acids with an N-terminal formyl group and a C-terminal ethanolamine (Table 1; Sarges and Witkop, 1965). Conventional gA channels are formed when opposing RH $\beta^{6.3}$-helical monomers are joined at their formyl-NH termini by six intermolecular hydrogen bonds (Fig. 1). The peptide backbone amide hydrogen atoms of residues 1, 3, and 5 of one monomer hydrogen bond with the carbonyl oxygen atoms of residues 5, 3, and 1, respectively, of the opposing monomer, and vice versa (Koeppe et al., 1994a). Channels formed by gA in membranes have a conformation that is not found outside of lipid bilayer membranes or membrane-like environments (Wallace et al., 1981; Wallace and Ravikumar, 1988; Langs, 1988; Bystrov and Arseniev, 1988; Abdul-Manan and Hinton, 1994; Cotten et al., 1999). The well-defined conformation of gA channels in lipid bilayers provides a way in which to examine the structural consequences of sequence modifications.

The preference for the formation of a RH conformation for gA channels has been previously investigated (Koeppe et al., 1992, 1994a; Providence et al., 1995). The contribution of the three central valine residues (Table 1) to the formation of the RH conformation was examined by executing a one-residue shift toward the N-terminus (Koeppe et al., 1994a). The resulting [Val^5, D-Ala^8]gA retained the RH SS $\beta^{6.3}$-helical conformation. This conservative modification resulted in the formation of channels with reduced ion conductance and channel duration. The reduced single-channel duration was attributed to a steric conflict between Val^1 in one monomer and Val^5 in the other monomer created by the one-residue shift. A modification of the

Received for publication 21 December 1998 and in final form 15 July 1999.

Address reprint requests to Dr. Roger E. Koeppe II, University of Arkansas, 103 Chemistry Building, Fayetteville, AR 72701. Tel.: 501-575-4976; Fax: 501-575-4049; E-mail: rk2@uafsysb.uark.edu.

Abbreviations used: gA, gramicidin A; CD, circular dichroism; DMPC, dimyristoylphosphatidylcholine; DPhPC, diphytanoylphosphatidylcholine; HOD, monodeuterated water; NMR, nuclear magnetic resonance; QCC, quadrupolar coupling constant; RH, right-handed; SDS, sodium dodecyl sulfate; SS, single-stranded.

0006-3495/99/10/1927/09 $2.00

TABLE 1 Sequences of native gA and [Val^5, D-Ala^8]gA using one-letter abbreviations.

Analog	Sequence
gA	HCO-V-G-A-L-A^5-V-V-V-W-L^{10}-W-L-W-L-W^{15}-NHCH$_2$CH$_2$OH
[Val^5, D-Ala^8]gA	HCO-V-G-A-L-V^5-V-V-A-W-L^{10}-W-L-W-L-W^{15}-NHCH$_2$CH$_2$OH

D-residues in each sequence are underlined. d_8-Val was incorporated at 1 or 7 in gA and at 1, 5, or 7 in [Val^5, D-Ala^8]gA.

orientation and motion of Val^1 may in turn affect Val^7 of the same monomer due to intramolecular interactions (Fig. 1).

To further investigate this issue, we have incorporated deuterium (^{2}H) labels at Val 1, 5, or 7 in [Val^5, D-Ala^8]gA. ^{2}H-NMR spectra of oriented and nonoriented samples in hydrated DMPC have been recorded. This technique allows the orientations and motions of the labeled valines to be estimated and compared to native gA.

Gramicidin A may also be used as a model to study the effects of acylation on integral membrane proteins because it occurs naturally in both free and acylated forms (Koeppe et al., 1985), and the acyl chain interacts sterically with Trp^9 and D-Leu^{10} (Koeppe et al., 1995, 1996). To better understand acylation effects, deuterated [Val^5, D-Ala^8]gA analogs were palmitoylated and ^{2}H-NMR spectroscopy was again performed. The results indicate that the covalent attachment of a fatty acid to the ethanolamine of [Val^5, D-Ala^8]gA does not significantly influence Val^1, Val^5, or Val^7.

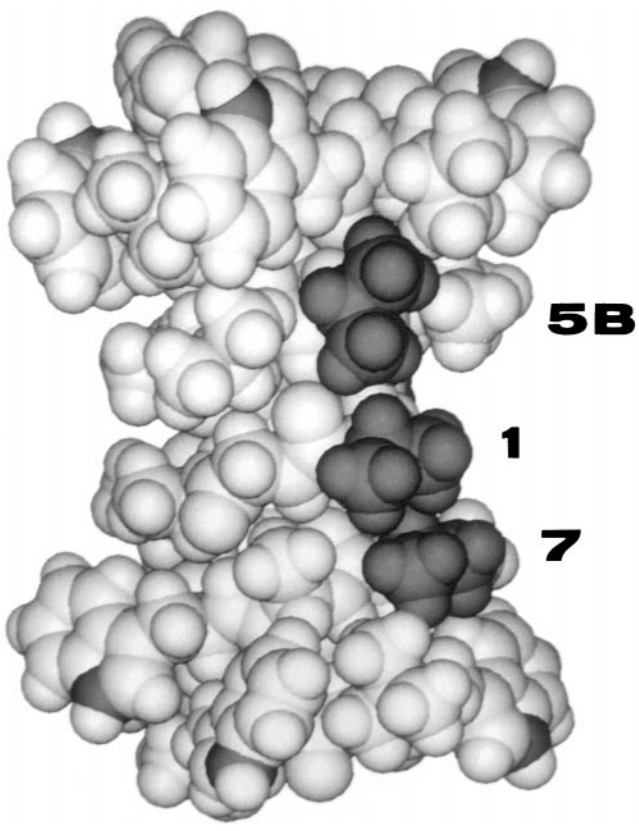

FIGURE 1 CPK model to illustrate the proximity of the side chains (highlighted in dark, and labeled) of valines 7 and 1 on one subunit, and the newly introduced 5-B on the other subunit, of a [Val^5, D-Ala^8]gA channel. In this energy-minimized model (not yet fit to NMR data), the side-chain χ_1 angles are illustrated at 64°, 182°, and 180° for valines 5-B, 1, and 7, respectively, top to bottom.

MATERIALS AND METHODS

Formyl-L-Val, non-deuterated Fmoc amino acids, and Fmoc-L-Trp resin for peptide synthesis were from Bachem (King of Prussia, PA), Peninsula Labs (Belmont, CA), and Advanced Chemtech (Louisville, KY). Deuterated L-Val was purchased from Cambridge Isotope Labs (Andover, MA). Deuterated L-Val was converted to the Fmoc derivative, and peptides specifically labeled at either valine 1, 5, or 7 in [Val^5, D-Ala^8]gA were prepared by previously described methods (Greathouse et al., 1999). Fifty milligrams of each specifically labeled [Val^5, D-Ala^8]gA was acylated and purified using previous methods (Koeppe et al., 1996).

Oriented and nonoriented samples containing 10:1 DMPC/gramicidin were prepared with ^{2}H-depleted H_2O as described in Koeppe et al. (1996). Cuvettes with oriented samples at 40% hydration were sealed with glass lids and epoxy. Control-oriented lipid samples from which gramicidin was omitted gave spectra with only a small sharp peak at 0 Hz attributable to HOD. Centrifuged, cut glass tubes that contained nonoriented samples with excess H_2O were sealed only with stoppers and parafilm, and so were more susceptible to contamination from atmospheric HOD.

^{2}H-NMR spectra were recorded as previously described (Koeppe et al., 1996), on a Bruker AMX 300 spectrometer modified for wideline operation with a 7.5-mm-diameter solenoid coil. Spectra were recorded using the quadrupolar echo sequence with full phase cycling (Davis et al., 1976), a 3.0-μs 90° pulse, a 30- or 100-ms interpulse time, and 0.9–1.5 million scans. The echo delay time was varied from 30 to 75 μs. A line broadening of 200 Hz for oriented samples, or 3000 Hz for nonoriented samples at 4°C, was applied to increase the signal-to-noise ratio.

To estimate the orientations and dynamics of the valine side chains both oriented and nonoriented samples were analyzed. Powder spectra for nonoriented samples at 4°C were simulated using the Fortran program MXQET (Greenfield et al., 1987), which has kindly been made available by Professor Robert L. Vold (http://nmr.physics.wm.edu). All simulated spectra were calculated on a Silicon Graphics O_2 workstation and were corrected for finite pulse length and echo delay. Single- and double-precision calculations gave identical results for the "hopping" regimes considered here. Angles of 70° (the tetrahedral supplement) between the deuterated (methyl) site and the hopping (C_α-C_β) axis, and of 120° between respective jump sites, were used. The site occupancies, exchange rates, and quadrupolar coupling constants were varied in the calculations. As has been done previously, the asymmetry parameter η was approximated as zero (Lee and Cross, 1994; Lee et al., 1995).

For the analysis of spectra from oriented samples at higher temperatures, the quadrupolar splittings ($\Delta\nu_q$ values) were converted to C-^{2}H bond orientation angles using the relation (Killian et al., 1992):

$$\Delta\nu_q = (3/2)(e^2qQ/h)(\tfrac{1}{2}[3\cos^2\theta - 1]) \cdot (\tfrac{1}{2}[3\cos^2\xi - 1])(\tfrac{1}{2}[3\cos^2\beta - 1]),$$

in which e^2qQ/h is the quadrupolar coupling constant (~168 kHz for C-^{2}H bonds), θ is the angle between the C-^{2}H or C-CD_3 bond and the membrane normal, β is the angle between the membrane normal and magnetic field, either parallel ($\beta = 0°$) or perpendicular ($\beta = 90°$), and ξ is either 0° for the Cα and Cβ deuterons or ~109.5° in the case of the tetrahedral geometry for the valine methyls (Killian et al., 1992).

For a starting atomic model, the "residue replace" function of InsightII (Biosym) was used to convert a gA model (Koeppe et al., 1996) to [Val^5, D-Ala^8]gA. With χ_1 set initially to 180° for Val^1 and Val^7—and to 60°, 180°, or 300° for Val^5—the model was energy-minimized successfully as described by Killian et al. (1992). In all test cases, the initial valine orientations changed little during the minimization, indicating that each starting position was allowable and free of serious steric conflicts. The backbone of one of these structures—that where χ_1 was near 60° for Val^5—was used to generate Fig. 1, and the same backbone was used to fit the deuterium NMR data. On this backbone, the valine side chains were allowed to rotate through 360°. Analysis began with the implementation of previous software, which rotates a given side chain about the Cα-Cβ bond (χ_1 torsion angle) in 0.5° increments (Koeppe et al., 1994b). At every interval in χ_1, the calculated $\Delta\nu_q$ values were compared to experimental results. As determined previously for Val^1 (Killian et al., 1992; Lee and Cross, 1994; Lee et al., 1995), this method resulted in no static solutions for any of the L-Val side chains that were examined.

A second method was then used to allow each valine to hop rapidly between any two χ_1 endpoints near 60°, 180°, or 300° (with tolerances of ±10°). This hopping is consistent with the data and simulations for cooled, nonoriented samples; see below. For rapid hopping, the calculated $\Delta\nu_q$ is the occupancy-weighted average of the individual values for the different states. Fractional occupancies of the two states were varied from 0 to 100% in 1% intervals, and the rms deviations between the theoretical and experimentally obtained $\Delta\nu_q$ values for each valine were minimized. This approach can be considered a subset of a generalized three-state model, in which one of the occupancies is close to zero. Rapid averaging of two states in all cases was sufficient to fit the data from oriented as well as nonoriented samples.

RESULTS

^{2}H-NMR measurements of nonoriented samples

Spectra were recorded at 4°C for individually deuterated valine 1, 5, or 7 [Val^5, D-Ala^8]gA samples in hydrated DMPC bilayers. By lowering the temperature below the gel-to-liquid crystalline phase transition point, global motion about the helix channel axis is eliminated (Cornell, 1987; Nicholson et al., 1987). Due to the "freezing out" of the global motions, local methyl group motions dominate the spectra in the region of −40 to +40 kHz (Lee et al., 1995). Fig. 2 shows the ^{2}H-NMR powder pattern spectra of each individually labeled valine at low temperature, together with spectral simulations. In each case the central sharp peak is an experimental artifact that is not seen with such intensity in the simulations (see also Lee and Cross, 1994). The ^{2}H-NMR powder pattern spectrum for d_8-Val^1 in [Val^5, D-Ala^8]gA is broad and flattened with distinct shoulders that appear intermediate between a single hump and a Pake pattern. The result suggests that the local motions of Val^1 have been slowed to an intermediate rate of side-chain hopping, as compared to Val^1 in native gA (Lee et al., 1995). Indeed, the spectrum for Val^1 in [Val^5, D-Ala^8]gA (Fig. 2 *A*) can be simulated nicely using a two-state model with relative occupancies of 0.7 and 0.3, an exchange rate of 5×10^4 s^{-1}, and a QCC of 49–50 kHz (Fig. 2 *B*).

The results for Val^1 in [Val^5, D-Ala^8]gA should be compared with the findings of Lee and Cross (1994), who have fit Val^1 in gA using a two-state (0.7, 0.3) model with QCC of 40 kHz and exchange rate of 10^6, or a three-state model with QCC of 46 kHz and exchange rate of 6.7×10^5. The QCC of ~168 kHz for a static C-^{2}H bond (Burnett and Muller, 1971) is reduced to 168/3 = 56 kHz by methyl rotation, and is further reduced by ~8% due to backbone librational averaging (Hing et al., 1990; Prosser et al., 1991; Killian et al., 1992). The theoretical maximum QCC for a side-chain methyl in a bilayer-incorporated gramicidin channel is therefore ~51 kHz. This value agrees with data for alanine-d_4 labeled gramicidin (Lee et al., 1993) and could be further reduced for valines by additional side-chain motions (Lee and Cross, 1994).

Compared to gA (at 4°C), we find a higher QCC and a 10–20-fold slower hopping rate for the Val^1 side chain in [Val^5, D-Ala^8]gA. A QCC of 49 kHz was sufficient to fit not

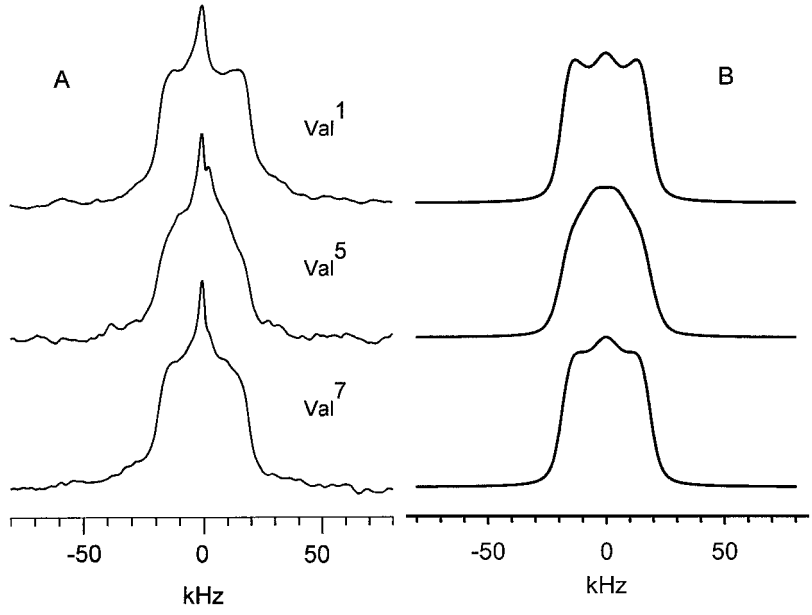

FIGURE 2 Experimental (*A*) and simulated (*B*) ^{2}H-NMR spectra of nonoriented samples of labeled Val^1 (*top*), Val^5 (*middle*), or Val^7 (*bottom*) in [Val^5, D-Ala^8]gA, hydrated in DMPC at 10:1 lipid/peptide; 4°C. The echo delay time is 75 μs and is accounted for in the simulations. The center peak at 0 Hz is attributed to residual HOD and is not simulated. The simulated spectra in (*B*) were calculated using a two-site model with occupancies of (0.7, 0.3) and jump times of 5×10^4, 3×10^5, and 8×10^4 s^{-1} for valines 1, 5, and 7, respectively.

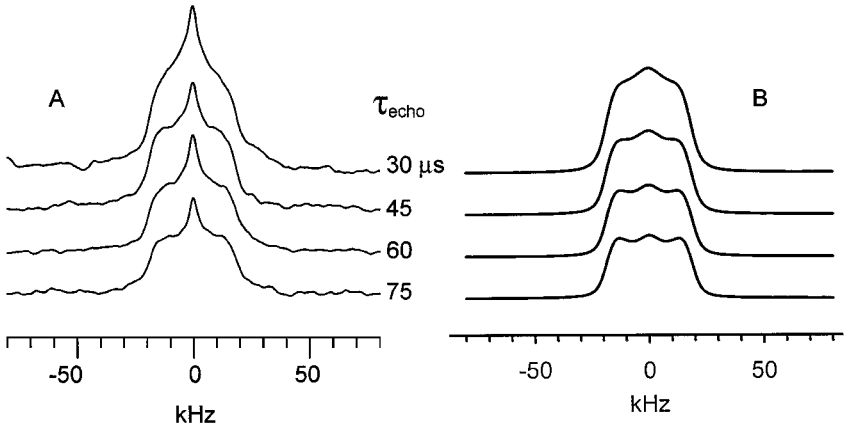

FIGURE 3 Experimental (*A*) and simulated (*B*) ^{2}H-NMR spectra of a nonoriented sample of labeled Val^1 in [Val^5, D-Ala^8]gA in DMPC at 4°C, as a function of the echo delay time, τ_{echo}. The peak at 0 Hz is attributed to residual HOD and is not simulated. The simulated spectra in (*B*) were calculated using a two-site model with occupancies of (0.7, 0.3) and a jump time of 5×10^4.

only Val^1 but also Val^5 and Val^7 in [Val^5, D-Ala^8]gA (Fig. 2), and the value of QCC was independent of the experimental echo delay (see below). The hopping rates for Val^7 and Val^5 are somewhat faster than Val^1 in [Val^5, D-Ala^8]gA, being 8×10^4 and at least 3×10^5, respectively, at 4°C (Fig. 2).

The hopping rates for Val^1 and Val^7 in [Val^5, D-Ala^8]gA are in a range that should be sensitive to the experimental echo delay time, τ_{echo}. This is indeed the case, as is illustrated for Val^1 in Fig. 3. For echo delays of 30–75 μs, the spectral shapes varied, but each spectrum could be simulated using the same QCC of 49 kHz and exchange rate of 5×10^4 as used in Fig. 2. By contrast, the more rapid hopping of Val^1 in gA (Lee and Cross, 1994) was insensitive to τ_{echo} between 30 and 75 μs (simulations not shown).

In [Val^5, D-Ala^8]gA, the side-chain hopping rate (at 4°C) increases in the order Val^1 < Val^7 < Val^5. In comparison to native gA, the introduction of Val^5 slows the hopping rate of Val^7 by about one order of magnitude and of Val^1 to a somewhat greater extent.

^{2}H-NMR measurements of oriented samples and comparison to native gA

^{2}H-NMR spectra of [Val^5, D-Ala^8]gA deuterated at position 1, 5, or 7 in oriented DMPC bilayers were recorded at several temperatures, echo delays, and sample orientations. Fig. 4 shows results for Val^1 at different values of τ_{echo}. Fig. 5 shows results for all three valines at 50°C and $\beta = 90°$. As for gA (Hing et al., 1990; Prosser et al., 1991; Killian et al., 1992; Ketchem et al., 1993), each of the backbone C_α-^{2}H quadrupolar splittings ($\Delta\nu_q$) for [Val^5, D-Ala^8]gA are found between 100 and 105 kHz at $\beta = 90°$ (Fig. 5), characteristic of the $\beta^{6.3}$ helix. There is no significant change in the peptide backbone conformation, thus confirming earlier conclusions that were based on circular dichroism, ^{1}H-NMR, and hybrid channel results (Koeppe et al., 1994a). The backbone C_α-^{2}H quadrupolar splittings in [Val^5, D-Ala^8]gA exhibit no significant change from their counterparts in native gA (Table 2).

The methyl deuterons undergo very fast motional averaging of the CD_3 top, which results in a small $\Delta\nu_q$ value and large intensity. The remaining spectral component with low intensity and intermediate $\Delta\nu_q$ then in each case can be assigned to the C_β-^{2}H (Killian et al., 1992; Lee and Cross, 1994). The spectra of Val^1 and Val^7 reveal a distinct spectral component with $\Delta\nu_q$ of 84 and 80 kHz, respectively, values that are significantly increased from those of Val^1 and Val^7 C_β-^{2}H in native gA (Table 2). The C_β-^{2}H peak for Val^5 in [Val^5, D-Ala^8]gA is less clear, but we make a

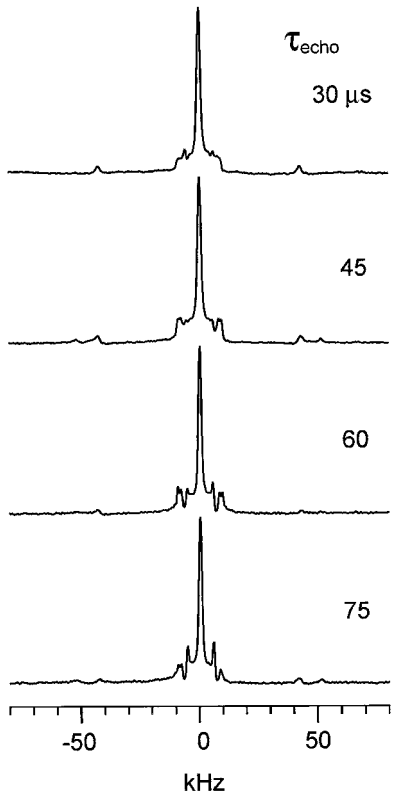

FIGURE 4 ^{2}H-NMR spectra as a function of the echo delay for an oriented sample of labeled Val^1 in [Val^5, D-Ala^8]gA, hydrated in DMPC at 10:1 lipid/peptide; 50°C; $\beta = 90°$.

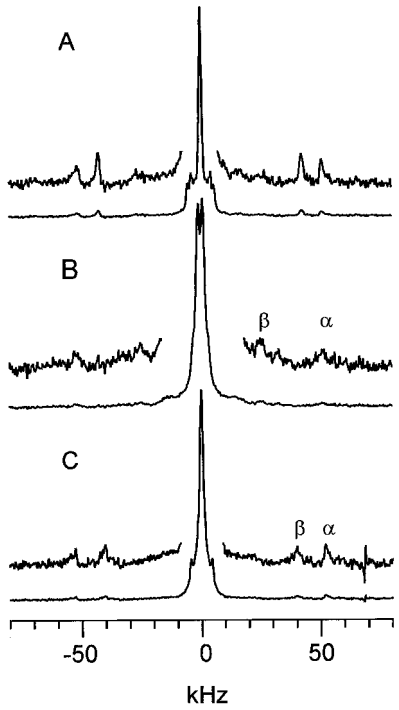

FIGURE 5 ^{2}H-NMR spectra of oriented samples of labeled Val^1 (*A*), Val^5 (*B*), or Val^7 (*C*) in [Val^5, D-Ala^8]gA, hydrated in DMPC at 10:1 lipid/peptide; 50°C; $\beta = 90°$. Vertical expansions show peaks from the deuterons on the α and β carbons.

tentative assignment to a $\Delta\nu_q$ near 50 kHz for a rather broad feature in Fig. 5 *B*. This is not an unreasonable assignment for a valine C_β-^{2}H, since the C_β-^{2}H of Val^7 in free and acylated gA has $\Delta\nu_q$ of 39 and 35 kHz, respectively (Table 2; Koeppe et al., 1995).

That distinct resonances are observed when $\beta = 90°$ confirms that the helix is undergoing fast axial reorientation. When samples are turned to $\beta = 0°$, the $\Delta\nu_q$ values should increase by a factor of 2, and this is indeed observed for the methyl deuterons (Fig. 6). At $\beta = 0°$, the spectral lines assigned to C_α-^{2}H and C_β-^{2}H (Fig. 6) become broad and weak, as others have observed (Hing et al., 1990; Killian et al., 1992).

TABLE 2 Magnitudes of quadrupolar interactions for deuterated valines 1, 5, and 7 in [Val^5, D-Ala^8]gA, palmitoyl-[Val^5, D-Ala^8]gA, and corresponding sites in gA, at 50°C and $\beta = 90°$

Molecule	Site	$\Delta\nu_q$ (kHz) C_α-^{2}H	C_β-^{2}H	C_γ-Methyls
[Val^5, D-Ala^8]gA	Val^1	102	84	0.0, 7.8, 11.0
	Val^5	104	50	2.0
	Val^7	104	80	0.0, 9.0
palmitoyl-[Val^5, D-Ala^8]gA	Val^1	102	84	0.0, 6.2, 10.4
	Val^5	—*	—*	1.0, 2.0
	Val^7	106	80	0.0, 8.0
gA	Val$^{1\,\#}$	106	68	2.0, 9.7
	Val$^{7\,\S}$	103	39	2.0
palmitoyl-gA	Val^1	106	68	2.0, 9.7
	Val$^{7\,\S}$	102	35	2.5

The listed quadrupolar splittings are one-half of the $\Delta\nu_q$ values observed at $\beta = 0°$.
*Peaks not visible for $\Delta\nu_q$ assignment.
#Values in agreement with Killian et al. (1992).
§Values in agreement with Koeppe et al. (1995).

Val^1

The methyl deuterons of Val^1 in [Val^5, D-Ala^8]gA display a complicated spectral pattern that varies somewhat with τ_{echo} (Fig. 4). When $\tau_{echo} = 75$ μs, there are three measurable components that have $\Delta\nu_q$ of 0.0, 7.8, and 11.0 kHz (Table 2; Fig. 5 *A*). The complex spectral pattern of the γ deuterons is quite different from native gA, which has $\Delta\nu_q$ of 2.0 and 9.7 with no peak at 0.0 kHz (Killian et al., 1992; Lee and Cross, 1994). The presence of three or more peaks, one of which is intense and at zero Hz, and the loss of intensity and the variation with τ_{echo} for the nonzero $\Delta\nu_q$ values, indicate altered side-chain dynamics of Val^1 and some motions close to the time scale of τ_{echo}. Along with these observations, the $\Delta\nu_q$ for C_β-^{2}H increases from 68 kHz in gA to 84 kHz in [Val^5, D-Ala^8]gA.

Val^7

The methyl groups of Val^7 in [Val^5, D-Ala^8]gA exhibit two spectral components, one with a $\Delta\nu_q$ of 9.0 kHz and a much more intense component at 0.0 kHz (Fig. 5 *C*). The CD_3

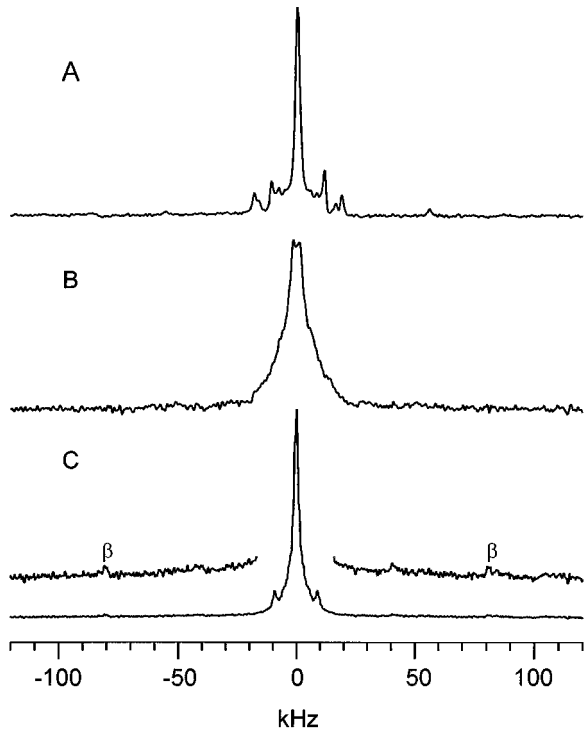

FIGURE 6 ^{2}H-NMR spectra at 50°C of oriented samples of labeled Val^1 (*A*), Val^5 (*B*), or Val^7 (*C*) in [Val^5, D-Ala^8]gA at $\beta = 0°$. The signals from the deuteron on Val^7-C_β are labeled in the expansion of spectrum (*C*).

values of Val[7] in native gA have a single $\Delta\nu_q$ of 2.0 kHz and a minor peak that has been attributed to a minor conformation. The peak associated with the minor conformation is absent after acylation of native gA (Koeppe et al., 1995). The changes in the $\Delta\nu_q$ values for Val[7] are less dramatic than for Val[1] in [Val[5], D-Ala[8]]gA, but nevertheless indicate that the side-chain properties have been altered somewhat, as compared to native gA. Another indication is the change in $\Delta\nu_q$ for C_β-^{2}H (Table 2).

Val[5]

The ^{2}H-NMR spectrum of d_8-Val[5] in [Val[5], D-Ala[8]]gA does not exhibit as clearly defined spectral components as seen for the deuterated Val[1] and Val[7] analogs (Fig. 5). With repeated samples, we have not been able to obtain a spectrum with distinct C_α-^{2}H and C_β-^{2}H peaks for Val[5]. This finding may be due to disordering of the backbone or side chain because of disruptive steric interactions (see Discussion). The Val[5] methyl groups give a peak with $\Delta\nu_q$ of 2.0 kHz and an additional broad component at the base of the main peak (Fig. 5 *B*). A comparison of Val[5] in [Val[5], D-Ala[8]]gA and gA is not possible, because Ala[5] is the counterpart in native gA (Table 1).

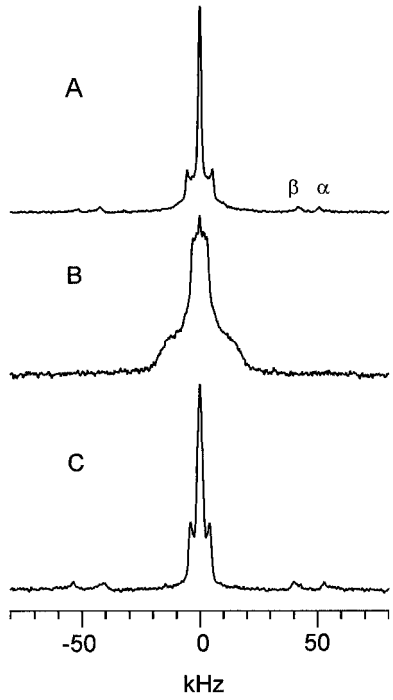

FIGURE 7 ^{2}H-NMR spectra at 50°C of oriented samples of labeled Val[1] (*A*), Val[5] (*B*), or Val[7] (*C*) in acyl-[Val[5], D-Ala[8]]gA at $\beta = 90°$. Peaks due to the deuterons on the α and β carbons are labeled in (*A*) and are also evident in (*C*).

Spectral changes after acylation

To determine whether or not covalently attached acyl chains influence residues positioned toward the middle of a [Val[5], D-Ala[8]]gA channel, the effects of acylation on the ^{2}H-NMR spectra were investigated. The spectrum of d_8-Val[1] in either gA (not shown) or [Val[5], D-Ala[8]]gA (Fig. 7 *A*) is not greatly affected by acylation. This result is not surprising since Val[1] is far from the acylation site on the ethanolamine (Koeppe et al., 1996).

Val[5] and Val[7] also are not much influenced by acylation. As before acylation, the spectrum of the acyl-[d_8-Val[5], D-Ala[8]]gA lacks spectral components that may be attributed to the C_α-^{2}H or C_β-^{2}H (Fig. 7 *B*). The methyl spectral component is difficult to interpret but appears to be comprised of multiple peaks and quite similar to the spectrum before acylation. The similarity of the Val[7] spectra before (Fig. 5 *C*) and after (Fig. 7 *C*) acylation is of particular interest due to the fact that when gA is acylated there is a small change in the $\Delta\nu_q$ of the C_β-^{2}H and a minor peak disappears; such changes do not occur for [Val[5], D-Ala[8]]gA.

Evaluation of side-chain rotameric states

The spectra of nonoriented samples at 4°C (Figs. 2 and 3) indicated (at least) two rotameric states with approximate occupancies of (0.7, 0.3) and respective exchange rates of 5×10^4, 3×10^5, and 8×10^4 for valines 1, 5, and 7 in [Val[5], D-Ala[8]]gA. Consistent with these results, the spectra of oriented samples at 50°C (Figs. 4 and 5) could not be fit by single static solutions for valine 1, 5, or 7. A second method of analysis was employed to allow the side chain to "hop" between two conformations (see Methods) and fit the observed $\Delta\nu_q$ values for the oriented samples. One expects that the exchange rates should be faster and the site occupancies may vary somewhat from the values at 4°C.

For Val[1] in [Val[5], D-Ala[8]]gA, the number, intensity, and arrangement of quadrupolar splittings are different from Val[1] of native gA (Table 2). The C_β-^{2}H $\Delta\nu_q$ (at $\beta = 90°$) has increased from 68 kHz in gA to 84 kHz in [Val[5], D-Ala[8]]gA. The Val[1] methyl deuterons in [Val[5], D-Ala[8]]gA give a strong peak at 0.0 kHz and less intense peaks near 7.8 and 11.0 kHz that are difficult to interpret. The spectral component at zero is too intense to be a contribution only from residual HOD. Analysis of the remaining non-zero spectral components (7.8 and 11.0 kHz) alone did not lead to any satisfactory two-state or three-state solutions. Separate analyses were then performed in which zero was one $\Delta\nu_q$ and the second $\Delta\nu_q$ was either 7.8 or 11.0 kHz. Both of these procedures resulted in two-state hopping models that gave good fits to experimental data with similar fractional occupancies. These results, together with the dependence on τ_{echo} (Fig. 4), suggest that Val[1] in [Val[5], D-Ala[8]]gA exists in several substates, each of which exhibits rapid two-state hopping about χ_1. The substates seem to be induced by the presence of Val[5]. Transitions among the substates exhibit complicated dynamics, for which we have insufficient information to make an interpretation.

Using quadrupolar splittings of 84 kHz for Cβ-^{2}H and (0.0, 11.0) for the methyls, the Val[1] dynamics fit nicely to

TABLE 3 Two-state hopping model, best fit χ_1 solutions and fractional occupancies of individually deuterated valine 1, 5, or 7 in [Val^5, D-Ala^8]gA

Site	Molecule	χ_1 Limits (°)	Fractional Occupancies
Val^1	gA*	(177 ± 120)	(0.78, 0.13, 0.09)
	[Val^5, D-Ala^8]gA	(185, 295), or	(0.88, 0.12)
		(175, 70)	(0.85, 0.15)
Val^5	[Val^5, D-Ala^8]gA	(175, 70), or	(0.65, 0.35)
		(190, 300)	(0.59, 0.41)
Val^7	gA*	(215 ± 120)	(0.61, 0.28, 0.11)
	[Val^5, D-Ala^8]gA	(185, 290)	(0.83, 0.17)

*Values taken from Lee et al. (1995), who used three-state models for the gA valines. Lee and Cross (1994) have also fit Val^1 in gA with a two-state model and occupancies of (0.7, 0.3). A two-state model is a specialized subset of a generalized three-state model with one fewer parameter (because one of the occupancies is close to zero). Three-state models are plausible for the valines of [Val^5, D-Ala^8]gA, and our data neither exclude nor require a three-state model for any of them.

two-state hopping about χ_1 between 185° (88% occupancy) and −65° (12% occupancy), or between 175° (85% occupancy) and +70° (15% occupancy; Table 3). For both fits, the sum of squared deviations between observed and calculated values is <1%. A graphical representation of these solutions is shown in Fig. 8. Similar results, with slightly different fractional occupancies, were obtained using splittings of (0.0, 7.8) kHz for the Val^1 methyls. These results agree well with the conclusions from the powder patterns at 4°C (above), except that the hopping rates are faster and the occupancy of the major state is increased from ~70% to ~85% at 50°C. The conclusions would not be significantly altered by considering a three-state model.

The quadrupolar splittings of Val^5 and Val^7 (Table 2) were similarly fit to describe the rotameric states of these valines in [Val^5, D-Ala^8]gA. Once again, two-state models were sufficient to reproduce the experimental data with low sums of squared deviations (below 1%). For Val^7, the fractional occupancy when χ_1 is near 180° (83%) is close to that for Val^1. Val^5 also has a major conformation with χ_1 in the vicinity of 180°, albeit with a lower occupancy (Table 3).

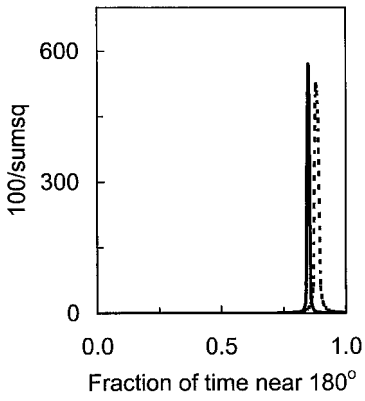

FIGURE 8 Two different fits to the ^{2}H-NMR data based on rapid two-state hopping of the side chain of Val^1 in [Val^5, D-Ala^8]gA: *solid line*, hopping between χ_1 of 175° and 70°; *dashed line*, hopping between 185° and 295°. "Sumsq" denotes the sum of squared deviations between observed and calculated $\Delta\nu_q$ values (see Methods).

DISCUSSION

[Val^5, D-Ala^8]gA was synthesized to test the influence of the central valines upon the helix sense of gA channels (Koeppe et al., 1994a). Gramicidin A and [Val^5, D-Ala^8]gA are true sequence isomers, in which only a single valine and a single alanine have been interchanged in the sequence. The D-Val^6-L-Val^7-D-Val^8 sequence in gA is shifted to L-Val^5-D-Val^6-L-Val^7 in [Val^5, D-Ala^8]gA. This change does not alter the RH helix sense of gramicidin channels in DMPC or DPhPC membranes, or in SDS micelles, as has been shown by CD spectroscopy, hybrid channel analysis, and two-dimensional NMR (Koeppe et al., 1994a). Single channels formed by [Val^5, D-Ala^8]gA exhibit ~0.55 of the Na^+ conductance of gA channels and have an average duration that is ~0.45 that of gA channels.

When a RH gA channel assembles within a phospholipid membrane (O'Connell et al., 1990), the transmembrane dimer is stabilized by six hydrogen bonds that link the backbone carbonyl and NH groups of residues 1—5, 3—3, and 5—1, respectively. The opposing side chains of these residues in the gA dimer are Val^1—Ala^5 and Ala^3—Ala^3 (Fig. 9). A significant packing change in [Val^5, D-Ala^8]gA is that Val^5 in one component monomer will now oppose Val^1 in the other to give the interactions Val^1—Val^5 along with Ala^3—Ala^3 (Fig. 9). It has been suggested that steric interference between the side chains of Val^1 and Val^5 could

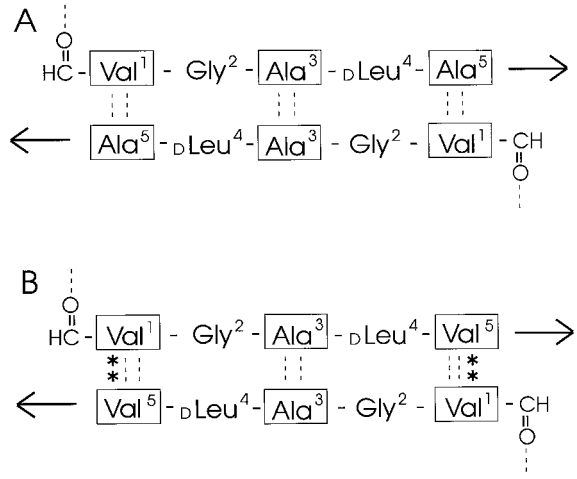

FIGURE 9 Schematic representations of the hydrogen bonding at the subunit junction in channels formed by (*A*) gA and (*B*) [Val^5, D-Ala^8]gA. L-amino acids are enclosed in boxes, whereas D-amino acids are not. The arrows represent the directions for continuing each helical subunit. In RH gA helices, the formyl groups participate in intramolecular hydrogen bonds (C═O- - -). Each dimer is stabilized by six intermolecular hydrogen bonds (- - -) that link the C═O and N–H groups, respectively, of residues 1/5, 3/3, and 5/1 of the component monomers. Single-channel data as well as ^{2}H-NMR spectra indicate that some steric interference between the Val^1 and Val^5 side chains (* *) modulates the properties of [Val^5, D-Ala^8]gA channels.

account for the altered single-channel properties of [Val^5, D-Ala^8]gA (Koeppe et al., 1994a). Furthermore, Val^7 sits above Val^1 in the next helical turn of the same monomer in the RH channel, and so it is plausible that a Val^1—Val^5 interaction, across the dimer junction, could be propagated into a secondary effect on Val^7. In this paper we have used specific deuterium labeling and ^{2}H-NMR spectroscopy to examine the average orientations and dynamics of the side chains of valines 1, 5, and 7 in [Val^5, D-Ala^8]gA, in order to make comparisons with the properties of valines 1 and 7 in gA.

Valine orientations and dynamics

Val^5

We will begin by discussing the newly introduced Val^5, which is not present in gA. Of the three valines, Val^5 undergoes the most rapid hopping in [Val^5, D-Ala^8]gA. At 4°C, we estimate the hopping rate to be at least 3×10^5 s^{-1} from the simulation in Fig. 2 *B*, and at 50°C the hopping should be faster. Nevertheless, the rate at 4°C is slower than has been estimated for Val^1 in native gA (Lee and Cross, 1994). Val^5 also exhibits a lower $\Delta\nu_q$ of 50 kHz for the C_β-^{2}H (Fig. 5 and Table 2). The analyses of spectra from both oriented and nonoriented samples (Figs. 2 and 5) indicate that a two-state model can fit the data, with rapid hopping of the Val^5 side chain about χ_1 between a rotamer near 180° (~60% occupancy) and another rotamer(s) near 60° and/or 300° (~40% occupancy; Table 3). The major conformation for Val^5 exists with lower occupancy at 180° than either Val^1 or Val^7 (see below). (We do not exclude a generalized three-state model in which each of the three canonical rotamers is populated with rapid dynamics, but either of the two-state models is sufficient to explain the data.)

Val^1 and Val^7 in [Val^5, D-Ala^8]gA as opposed to gA

In comparison to valines 1 and 7 in gA (Lee and Cross, 1994; Lee et al., 1995), and to Val^5 in [Val^5, D-Ala^8]gA, Val^1 and Val^7 exhibit slower (hindered) side-chain hopping motions at 4°C. Although the hopping rates should be faster at 50°C, the results nevertheless suggest a valine/valine steric interference (see Fig. 1). We note also that the $\Delta\nu_q$ values for the C_β-^{2}H increase from 39 to 80 kHz for Val^7 and from 68 to 84 kHz for Val^1 when Val^5 is introduced (Table 2).

In agreement with the fits to the side-chain hopping at 4°C, we find no static solutions for χ_1 for either Val^1 or Val^7 in [Val^5, D-Ala^8]gA at 50°C (Table 3). Adequate solutions were found that include two-state hopping on the NMR time scale and the occupancies were always above 80% for χ_1 near 180° (Table 3). For Val^1, the possible solutions in [Val^5, D-Ala^8]gA closely describe the fractional occupancies in gA also (albeit on a different time scale, as suggested by Fig. 2), whereas for Val^7 in [Val^5, D-Ala^8]gA the fraction of time spent with χ_1 near 180° is somewhat higher than in gA (an increase from ~60% to ~80%; Table 3).

A remaining puzzle is that the ^{2}H-NMR spectrum for Val^1 in oriented samples of [Val^5, D-Ala^8]gA (Fig. 4) exhibits multiple discrete quadrupolar splittings that vary somewhat with τ_{echo}, in addition to the strong peak at 0.0 Hz. Although a detailed interpretation is elusive, the spectra nevertheless suggest complicated dynamics on a time scale that is close to τ_{echo} as, for example, could be caused by a steric interference with the Val^5 side chain.

Effect of acylation on gA and [Val^5, D-Ala^8]gA

Previously, it was shown that Val^7 in gA has a major conformation in which the side chain undergoes rapid three-state hopping (Table 3; Lee et al., 1995) and a minor conformation that is represented by a minor additional quadrupolar splitting from the methyl groups (Koeppe et al., 1995). The minor peaks are not an artifact because they are observed whether samples are oriented at $\beta = 0°$ or 90°, and in spectra from independent samples in two different laboratories (Koeppe et al., 1995; Lee et al., 1995). When gA is acylated, there is no change in the major conformation of Val^7, but the minor conformation disappears (Koeppe et al., 1995). We now report also that the ^{2}H-NMR spectrum of Val^1 in gA after acylation is identical to that before acylation (Table 2; figure not shown).

For acyl [Val^5, D-Ala^8]gA, the ^{2}H-NMR spectra (Fig. 7) suggest only small changes in the dynamics of valines 1, 5, and 7, but no large changes in the major conformation of any of the valines following acylation. The change in the pattern of minor peaks for the methyls of Val^1 after acylation (compare Figs. 5 *A* and 7 *A*) is reminiscent of Val^7 in gA. For Val^7 in [Val^5, D-Ala^8]gA, the relative intensity of the peaks with $\Delta\nu_q$ of 8 kHz increases after acylation (Fig. 7 *C*). These effects could be caused by changes in the side-chain dynamics. The major finding, however, is that acylation has very little effect on the properties of valines 1 and 7 in gA or of valine 1, 5, and 7 in [Val^5, D-Ala^8]gA. The results are consistent with the earlier finding that the acyl chains are largely on the same side of a gramicidin channel dimer, where they each pass near the side chains of residues 9 and 10 of their respective subunits (see Fig. 7 of Koeppe et al., 1996). In this location, the acyl chains are radially ~140–180° away from the Val^7-Val^1-Val^{5B} "triad" of Fig. 1.

CONCLUSION

Deuterium NMR spectra show that for the gramicidin sequence isomer [Val^5, D-Ala^8]gA in phospholipid membranes, the backbone folding is unchanged. Interactions with valine 5 slow the motions of the valine 1 and 7 side chains and correlate with altered single-channel properties. Acylation of [Val^5, D-Ala^8]gA affects these valines very little.

We thank Olaf Andersen and Antoinette Killian for helpful discussions. We are grateful to two helpful reviewers and to Editorial Board Member Timothy Cross for the assistance that they have provided. We thank Professor Robert L. Vold for making available the program MXQET at http://nmr.physics.wm.edu.

This work was supported in part by Grant MCB-9816063 from the National Science Foundation.

REFERENCES

Abdul-Manan, Z., and J. F. Hinton. 1994. Conformational states of gramicidin A along the pathway to the formation of channels in model membranes determined by 2D NMR and circular dichroism spectroscopy. *Biochemistry*. 33:6773–6783.

Andersen, O. S., and R. E. Koeppe II. 1992. Molecular determinants of channel function. *Physiol. Rev.* 72:S89–S158.

Becker, M. D., D. V. Greathouse, R. E. Koeppe II, and O. S. Andersen. 1991. Amino acid sequence modulation of gramicidin channel function: effects of tryptophan-to-phenylalanine substitutions on the single-channel conductance and duration. *Biochemistry*. 30:8830–8839.

Becker, M. D., R. E. Koeppe II, and O. S. Andersen. 1992. Amino acid substitutions and ion channel function. Model-dependent conclusions. *Biophys. J.* 62:25–27.

Burnett, L. J., and B. H. Muller. 1971. Deuterium quadrupole coupling constants in three solid deuterated paraffin hydrocarbons. *J. Chem. Phys.* 55:5829–5831.

Bystrov, V. F., and A. S. Arseniev. 1988. Diversity of the gramicidin A spatial structure: two-dimensional proton NMR study in solution. *Tetrahedron*. 44:925–940.

Cardew, G., and D. Chadwick. (Editors). 1999. Gramicidin and Related Ion Channel-Forming Peptides (Novartis Foundation Symposium 225). Wiley, Chichester, England.

Cornell, B. 1987. Gramicidin A-phospholipid model systems. *J. Bioenerg. Biomembr.* 19:655–676.

Cotten, M., R. Fu, and T. A. Cross. 1999. Solid-state NMR and hydrogen-deuterium exchange in a bilayer-solubilized peptide: structural and mechanistic implications. *Biophys. J.* 76:1179–1189.

Davis, J. H., K. R. Jeffrey, M. Bloom, M. I. Valio, and T. P. Higgs. 1976. Quadrupolar echo deuteron magnetic resonance spectroscopy in ordered hydrocarbon chains. *Chem. Phys. Lett.* 42:390–394.

Durkin, J. T., R. E. Koeppe II, and O. S. Andersen. 1990. Energetics of gramicidin hybrid channel formation as a test for structural equivalence. Side-chain substitutions in the native sequence. *J. Mol. Biol.* 211: 221–234.

Greathouse, D. V., R. E. Koeppe II, L. L. Providence, S. Shobana, and O. S. Andersen. 1999. Design and characterization of gramicidin channels. *Methods Enzymol.* 294:525–550.

Greenfield, M., A. Ronemus, R. Vold, R. Vold, P. Ellis, and T. Raidy. 1987. Deuterium quadrupole-echo NMR spectroscopy. III. Practical aspects of lineshape calculations for multiaxis rotational processes. *J. Magn. Reson.* 72:89–107.

Hing, A. W., S. P. Adams, D. F. Silbert, and R. E. Norberg. 1990. Deuterium NMR of Val$^1 \cdots$ (2-^{2}H)Ala$^3 \cdots$ gramicidin A in oriented DMPC bilayers. *Biochemistry*. 29:4144–4156.

Jude, A. R., D. V. Greathouse, R. E. Koeppe II, L. L. Providence, and O. S. Andersen. 1999. Modulation of gramicidin channel structure and function by the aliphatic "spacer" residues 10, 12 and 14 between the tryptophans. *Biochemistry*. 38:1030–1039.

Ketchem, R. R., W. Hu, and T. A. Cross. 1993. High-resolution of gramicidin A in a lipid bilayer by solid-state NMR. *Science*. 261: 1457–1460.

Killian, J. A. 1992. Gramicidin and gramicidin/lipid interactions. *Biochim. Biophys. Acta*. 1113:391–425.

Killian, J. A., M. J. Taylor, and R. E. Koeppe II. 1992. Orientation of the valine-1 side chain of the gramicidin transmembrane channel and implications for channel functioning. A 2H NMR study. *Biochemistry*. 31:11283–11290.

Koeppe, R. E. II, and O. S. Andersen. 1996. Engineering the gramicidin channel. *Annu. Rev. Biophys. Biomol. Struct.* 25:231–258.

Koeppe, R. E. II, D. V. Greathouse, A. Jude, G. Saberwal, L. L. Providence, and O. S. Andersen. 1994a. Helix sense of gramicidin channels as a "nonlocal" function of the primary sequence. *J. Biol. Chem.* 269: 12567–12576.

Koeppe, R. E. II, J. A. Killian, and D. V. Greathouse. 1994b. Orientations of the tryptophan 9 and 11 side chains of the gramicidin channel based on deuterium NMR spectroscopy. *Biophys. J.* 66:14–24.

Koeppe, R. E. II, J. A. Killian, T. C. B. Vogt, B. De Kruijff, M. J. Taylor, G. L. Mattice, and D. V. Greathouse. 1995. Palmitoylation-induced conformational changes of specific side chains in the gramicidin transmembrane channel. *Biochemistry*. 34:9299–9306.

Koeppe, R. E. II, J. A. Paczkowski, and W. L. Whaley. 1985. Gramicidin K, a new linear channel-forming gramicidin from *Bacillus brevis*. *Biochemistry*. 24:2822–2826.

Koeppe, R. E. II, L. L. Providence, D. V. Greathouse, F. Heitz, Y. Trudelle, N. Purdie, and O. S. Andersen. 1992. On the helix sense of gramicidin A single channels. *Proteins*. 12:49–62.

Koeppe, R. E. II, T. C. B. Vogt, D. V. Greathouse, J. A. Killian, and B. De Kruijff. 1996. Conformation of the acylation site of palmitoylgramicidin in lipid bilayers of dimyristoylphosphatidylcholine. *Biochemistry*. 35: 3641–3648.

Langs, D. A. 1988. Three-dimensional structure at 0.86 Å of the uncomplexed form of the transmembrane ion channel peptide gramicidin A. *Science*. 241:188–191.

Lee, K. C., and T. A. Cross. 1994. Side-chain structure and dynamics at the lipid-protein interface: Val-1 of the gramicidin A channel. *Biophys. J.* 66:1380–1387.

Lee, K. C., W. Hu, and T. A. Cross. 1993. ^{2}H-NMR determination of the global correlation time of the gramicidin channel in a lipid bilayer. *Biophys. J.* 65:1162–1167.

Lee, K. C., S. Huo, and T. A. Cross. 1995. Lipid-peptide interface: valine conformation and dynamics in the gramicidin channel. *Biochemistry*. 34:857–867.

Nicholson, L. K., F. Moll, T. E. Mixon, P. V. LoGrasso, J. C. Lay, and T. A. Cross. 1987. Solid-state nitrogen-15 NMR of oriented lipid bilayer bound gramicidin A. *Biochemistry*. 26:6621–6626.

O'Connell, A. M., R. E. Koeppe II, and O. S. Andersen. 1990. Kinetics of gramicidin channel formation in lipid bilayers: transmembrane monomer association. *Science*. 250:1256–1259.

Prosser, R. S., J. H. Davis, F. W. Dahlquist, and M. A. Lindorfer. 1991. Deuterium nuclear magnetic resonance of the gramicidin A backbone in a phospholipid bilayer. *Biochemistry*. 30:4687–4696.

Providence, L. L., O. S. Andersen, D. V. Greathouse, R. E. Koeppe II, and R. Bittman. 1995. Gramicidin channel function does not depend on phospholipid chirality. *Biochemistry*. 34:16404–16411.

Salom, D., M. C. Bañó, L. Braco, and C. Abad. 1995. HPLC demonstrates that an all Trp→Phe replacement in gramicidin A results in a conformational rearrangement from β-helical monomer to double-stranded dimer in model membranes. *Biochem. Biophys. Res. Commun.* 209: 466–473.

Salom, D., E. Pérez-payá, J. Pascal, and C. Abad. 1998. Environment- and sequence-dependent modulation of the double-stranded to single-stranded conformational transition of gramicidin A in membranes. *Biochemistry*. 37:14279–14291.

Sarges, R., and B. Witkop. 1965. Gramicidin A. V. The structure of valine- and isoleucine-gramicidin A. *J. Am. Chem. Soc.* 87:2011–2020.

Wallace, B. A., and K. Ravikumar. 1988. The gramicidin pore: crystal structure of a cesium complex. *Science*. 241:182–187.

Wallace, B. A., W. R. Veatch, and E. R. Blout. 1981. Conformation of gramicidin A in phospholipid vesicles: circular dichroism studies of effects of ion binding, chemical modification, and lipid structure. *Biochemistry*. 20:5754–5760.